International Information and Engineering Technology Association

Advancing the World of Information and Engineering

Preparation and Synthesis of SnS-Doped CdS Nanoparticles for Solar Cell Application

Zainab Qassim Mohamed[1], Safa Ahmed Jabbar[2], Khalid Haneen Abass[2*], Ban A. Naser[3]

[1] Iraq Ministry of Education, Baghdad 51001, Iraq
[2] Department of Physics, College of Education for Pure Sciences, University of Babylon, Babylon 51002, Iraq
[3] Department of Physics, College of Science, University of Babylon, Babylon 51002, Iraq

Corresponding Author Email: pure.khalid.haneen@uobabylon.edu.iq

ABSTRACT

An easy and applicable technique used to fabricate the nanoparticles of cadmium sulfide (CdS) via the thermal evaporation by annealing the samples at temperature 200℃ for one and two hours at thicknesses (50, 75, and 100) nm. The CdS nanoparticles are synthesized, and the wide uses in solar cells are discussed. Their average roughness and the square of mean root were studied by (AFM). The optical characteristic deals with observe the absorbance spectra using a UV-Visible spectrophotometer. By the change of thickness and decrease of the refractive index with increasing thickness, while the absorbance increased, could show the significantly effect of the optical properties. At the range of (200-1100 nm) Transmission data were analyzed. whereas decreased from (3.50 to 3.35 nm) the optical band gap. The energy gap with high values refer to the quantization effect. The absorption coefficient, the extinction coefficient increased with increasing thickness. The method of Z-scan applied for calculate the optics in nonlinear. An investigation used a diode pump solid state laser with varying laser powers (56, 70, 84, and 102) mW at a wavelength of 457 nm. For all produced samples, the results demonstrated that while the nonlinear absorption coefficient decreased as powers increased, the nonlinear refractive index increased. Comparing SnS nanofilms doped with various amounts of CdS nanomaterials, the latter have demonstrated superior nonlinear characteristics and optical limiting. Compared to the results of AFM and UV.

1. INTRODUCTION

The technique used in Nanotechnology is a cutting-edge technology which is come to be the first of the developing a wide applicable approach, attracting global notation and enhancing an important part in medical applications. Specifically, a nanoscale particle of semiconductor, when the blue line shifts with reducing particle diameter in the UV-Vis absorption high levels, becomes noticeable and comprehensible from the effect of size quantization [1]. A well-known band gap in direct position of SnSin normal situations about 2.4 eV [2-4]. Investigation throws the II–VI chalcogenide type of semiconductors has led a worldwide use, which is why it may produce nanostructured films for producing cutting-edge optoelectronic devices. CdS is classified as one of the most effective components of this family [5]. The devices such as Solar cells and photovoltaic cells, may in direct way convert solar energy into electricity [6]. For the purpose, the suitable energy gap of SnS can be more benefit with modifying the energy band gap [3, 7].

Despite that, it has a wide, flexible beginning for the absorption that occurred on optical, which agrees with the ideal band gap (E_g) with (1.1–1.5) eV, which may requisite in high-level efficiency corresponding with the Shokley-Queisser limit [8]. The element in transition position such as

Cadimium, showing perfect conductivity in electricity; it also enhances a fine resistance for oxidation. CdS Quantum Dots were introduced by the CdS material which exists as crystalline shape at colloidal fluorescent semiconducting. Nevertheless, the nanoparticles of CdS, Quantum Dots may well-known between described materials, because of superstitious electrical or optical characteristics, for future use at various fields like the bio-sensing, bio-imaging methods, solar cells, nano- medical applications, drug delivery, and molecular pathology [9].

The varied types of CdS Nanoparticles (NPs) by using several procedures were synthesized, including chemical, physical, and biological techniques [10]. For minimum clusters in case of a duplicated crystals in CdS, corresponding to UV-vis absorption and particle diameter, were attributed to the CdS nanoparticles molecular crystals that already mentioned. Latterly, excellent well-arranged colloidal films or crystals roughly as monodisperse CdSe NPs with diameters among (15-100) Å, that has agreed with the finding of Bawendi and the others [11].

An applicable p-type SnS semiconductor with electronic properties for photovoltaic characterizations exists in the noticeable range of the solar spectra. It has a high optical absorption coefficient (α) between (10^4-10^5 cm^{-1}) [12]. It can be used in various applications, such as light-emitting diodes

[13], logic circuits [5], and solar cells [8].

Recent publications reported the thermal evaporation synthesis in this study applied to fabricate the Nano films of CdS. Herein, the attention is concentrated the development of CdS multicrystalline Nano films by measuring on thermal evaporation which that, changes with the change of optical and structural properties. the UV-VIS model of the spectrophotometer was applied to the samples for synthesis. The optical spectrum is focused on calculating constants in optics, for example, the optical band gap, extinction coefficient, and refractive index. Most previous publications focused on producing CdS thin films with various procedures, like a chemical bath deposition (CBD) [14], spray pyrolysis method [15], electron beam vacuum evaporation [16], thermal evaporation [17], molecular beam epitaxy [18], liquid-phase deposition [19], pulsed laser deposition [20], and close space vapor transport (CSVT) [21]. That is why, SnS annealing has recently attracted good attention for changing their physical characteristic [22]. p-SnS widely enhanced in solar sell uses, such as an absorber substantial which involves a wide bandgap for the n-type semiconductor, for example, CdS, like a heterojunction accomplice. Most previous publications focused on that, the SnS absorber layer and Production of the open material of CdS, resulting in a difference between the CdS/SnS hetero-constructions produced a long time ago. A well-known efficiency in which the SnS/CdS nanofilm photovoltaic cells (TFSCs) about (1.3%) by Reddy et al. [23]. For synthesize the n-CdS/p-SnS heterojunction photovoltaic cell, a reverse contact electrode called molybdenum was sputtered on the p-SnS layer by the evaporation method (Edward C-306) as the rang of power about (50) W in time 10 min [24]. Due to a hassle-free and organized synthesis. While enhanced in this work various method which deals with producing CdS nano films via a thermal evaporation method.

2. EXPERIMENTAL SECTION

2.1 Preparation method of cadmium sulfide

The substrates made from glass or silicon were washed with clean water and ethanol to reduce surface contamination, then made it dry completely, and the material was then situated in a warm vanishing framework in a Molybdenum boat modified as (Edward C-306). Covered the chamber firmly and the vacuum over (1×10^{-7} mbar).the applications of thermal evaporator such as an electric resistance heater for to dissolve the material and increases vapor pressure enhancing a good properties, having been emptied of air, which could let the vapor to spread the substrate wanting reacting or scattering on the atoms such as the gas-phase inside chamber, also may avoid the absorption of impurities which caused by the remaining gas in the vacuum [25]. A weight of 0.06 g of CdS (90%) and SnS (10%) in a molybdenum boat was used to evaporate the powders. The prepared substrate was annealed for 2 hours at 200°C.

The substrate thickness measured by applying two different methods, one by measuring the optical characteristic of the nano substrate applies the reflectance technique, whereas others used the weight equation as reported in the following Eq. (1) [26]:
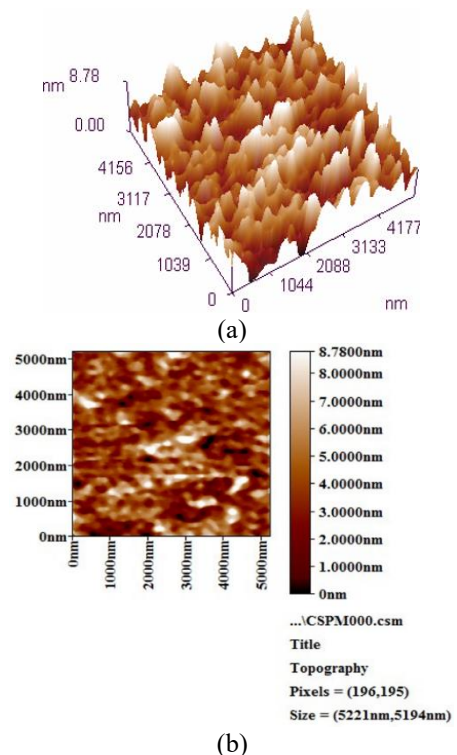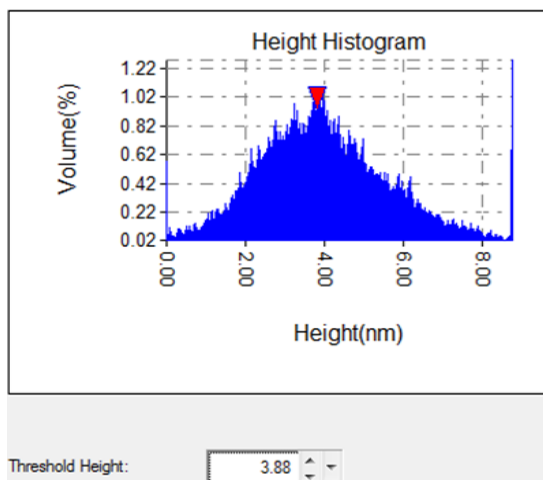
$$t = m/(2\pi\rho R^2) \qquad (1)$$

The film thickness (t) in nm, also (m) the material mass that evaporated in grams, (ρ) material density as (g/cm^3), the substrate and boat distance approximately about (15 cm), which is presented as (R). It was noticed that its approximately (50, 75, and 100) nm. By UV-Visible Spectrophotometer about (300-1100) nm, the optical properties have been examined.
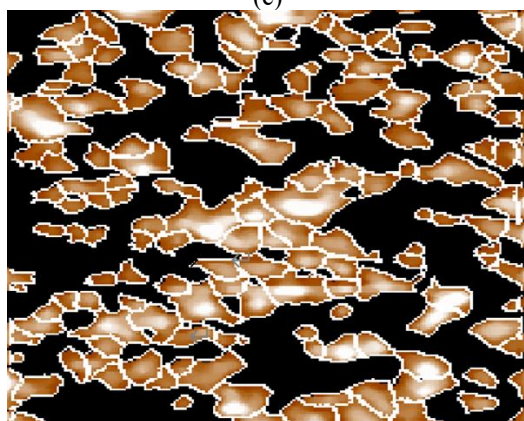
2.2 Results and discussion

By deposition the CdS nano films exhibited the morphology of the surface of the samples synthesized by a thermal evaporation technique, as reduce the pressure to (1×10^{-7}) mbar with percentage deposition equal to (0.3) nm/sec with various thickness was examined by AFM. The image surface in two- and three-dimension AFM, with granular distribution, and grain histogram thin films. The results of Figures 1-3 display an identical granular surface morphology. It can be observed from the figures that, increasing in both roughness as (1.35 nm to1.77 nm), also the square of mean root (1.72 - 2.26) nm as shown in Table 1. That show the results that agree with other researches [27]. The force among the atoms from the tip to the sample can be focused by atomic force microscopy that positioned between (0.1-100) nm [28].

From a plane of view images, may calculate the average grain diameter, which increased as of (305.7 - 310.2) nm for the prepared films. The ten-point height represent the surface morphology on the thin film, which refer to the height of ten points measured by AFM device. Which is in accordance with the findings of researches [28, 29]. They increase from (8.23 to 11.1) nm as in part (a)and (b) from the Figures 1-3 where (a) represents a picture in three dimensions and the highest level was a peak with a rate of (2.29-2.23) nm for the surfaces of these membranes, (b) represents a picture in two dimensions. Due to this results which includes the results refer to extremely noble caused a surface agglomeration, that appeared like singular grains. A grain height of small tens in nanometers was exposed by this tilted image, it's presented by Table 1.
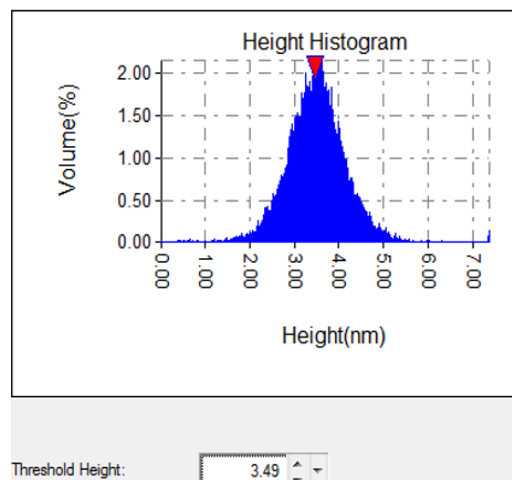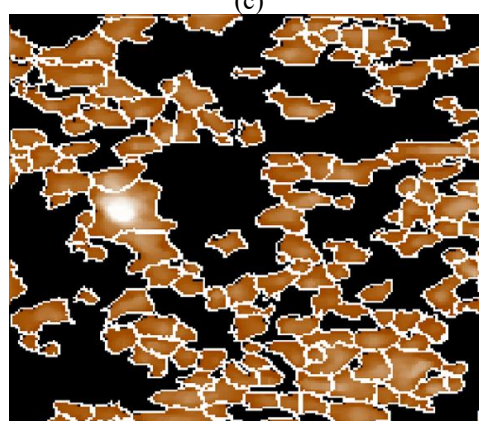

(a)

...\CSPM000.csm
Title
Topography
Pixels = (196,195)
Size = (5221nm,5194nm)

(b)

(c)

Threshold Height: 3.88

(c)

Threshold Height: 3.49

(d)

(d)

Figure 1. The AFM pictures of CdS:SnS thin film at thickness 50 nm, where (a) 3-D, (b) 2-D, (c) the whole numbers of particles, and (d) Grain Histogram
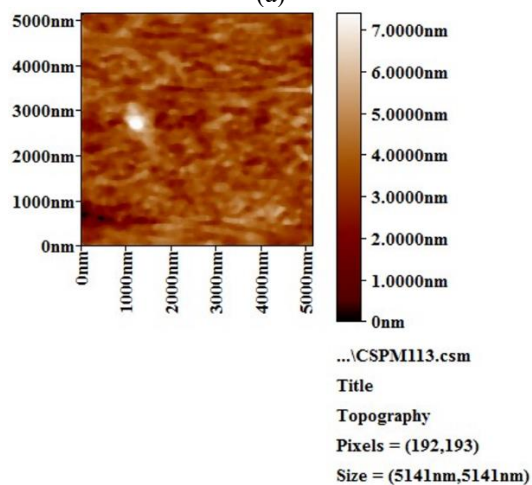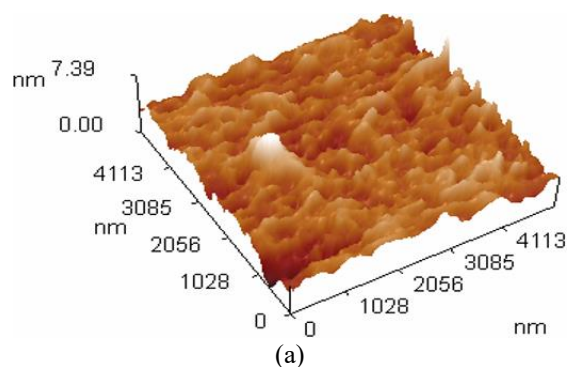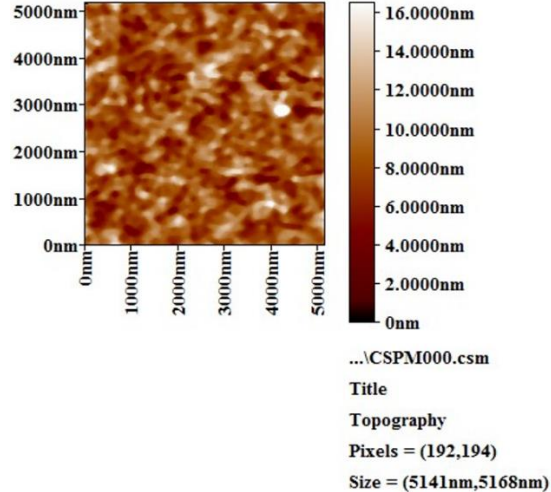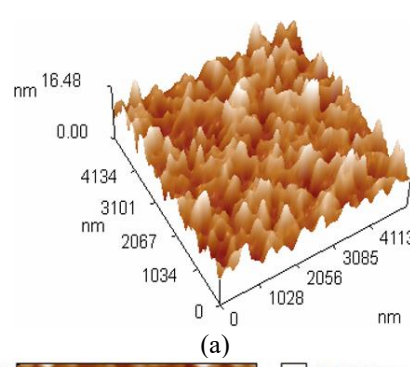
Figure 2. The AFM pictures of CdS:SnS nano film at thickness 75 nm, (a) 3-D, (b) 2-D, (c) the whole particles numbers, and (d) Grain Histogram

(a)

...\CSPM113.csm
Title
Topography
Pixels = (192,193)
Size = (5141nm,5141nm)

(b)

(a)

...\CSPM000.csm
Title
Topography
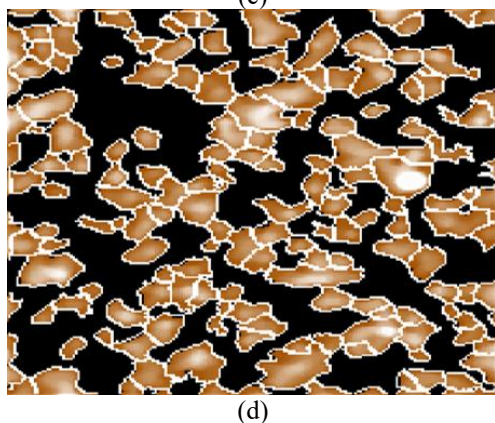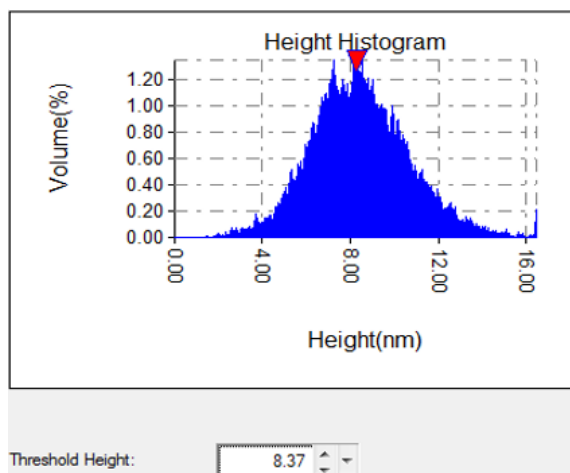Pixels = (192,194)
Size = (5141nm,5168nm)

(b)

(c)

(d)

Figure 3. The images of atomic force microscopy for CdS:SnS thin film at thickness 100 nm, where (a) 3-D, (b) 2-D, (c) the whole numbers of particles, and (d) Grain Histogram

Table 1. Morphological properties for CdS:SnS nanofilms at different thickness and a temperature of 200°C for 2 h

Type of Films	Average Roughness Sa (nm)	Root Mean Square Sq (nm)	Ten Point Height Sz (nm)	Average Diameter (nm)
CdS doping with SnS at a thickness of 50 nm	1.35	1.72	8.23	305.7
CdS doping with SnS at a thickness of 75 nm	0.525	0.0104	3.74	305.4
CdS doped by SnS at thickness 100 nm	1.77	2.26	11.1	310.2

3. THE LINEAR-OPTICAL PROPERTIES

3.1 The absorbance

After doping with SnS, it is shown that the absorbance is increasing after annealing temperature because of the increase in the material crystallization and decrease defects crystalline [29]. Noticed that shifting in absorption maxima to shorter wavelengths by decreasing particle diameter as result of the confinement increases for the photo produced charge carriers in tiny atoms. As well as, by decreases in size, the absorption spectra increased the constructed as the size decreased due to the changes in structure of the electronic band represented the molecular stages with indissoluble energy spacing. Figure 4 represents the correlation between the absorbance and the wavelength. As shown in Figure 4, absorbance increases as the thickness increase, which is corresponding to the number of particles may increase, also the number of collisions between the incident photons with the particles.
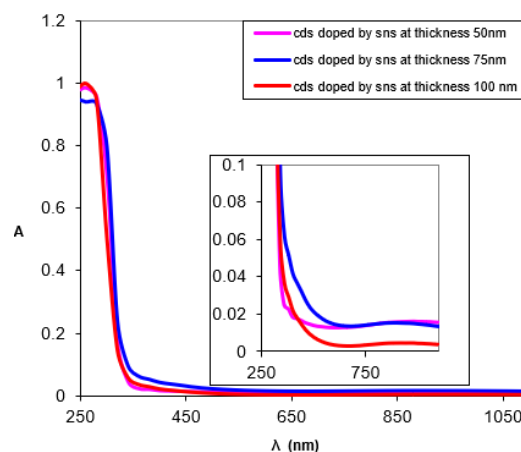

Figure 4. The spectra absorbance that varied with wavelength for CdS:SnS nanofilms with different thickness

3.2 The absorption coefficient (α)

The optical absorption coefficient represented by Figure 5 displays in relation to wavelength for the CdS:SnS film. To study the absorption coefficient spectra could represent the energy gap (E_g) among the valence band and the conduction band caused by a transition, which are divided into direct and indirect on both amorphous and crystalline components. It was observed that all the synthesized films have a great absorption coefficient ($\alpha > 10^4$ cm^{-1}), which denotes the increasing in the rate probability of a allowed transitions. This Character illustrates the absorption coefficient of the films increasing rapidly as the thickness increases.
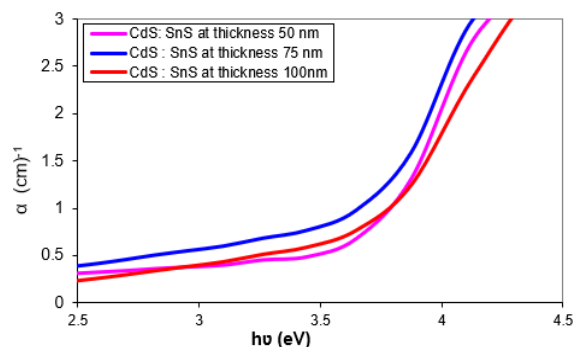

Figure 5. A scheme of absorption coefficient (α) relative to the energy of photon (hυ) of CdS:SnS at various thicknesses

3.3 The optical energy gap (Eg)

The CdS:SnS nano films optical energy gap is determined by using the Eq. (2) [30]:

$$\alpha h\upsilon = B \left(h\upsilon - E_g^{opt} \pm Eph\right)^n \qquad (2)$$

By significant the band parameter of the variable for the above equation, in which B represent a band tailing, n represent the parameter in which specifies the optical transition type for an investigated material, the indirect forbidden transitions (n = 3) while the direct allowed transitions (n=2). $(\alpha h v)^2$ scheme with the energy of incident photon (hv) shows a CdS:SnS substrate with type in direct transition as a semiconductor to nano films demonstrated in Figure 6. After annealing for two hours with various thicknesses of CdS doping with SnS for the prepared films are illustrated in Figure 6. the decrease in energy gap corresponding to this figure range (3.5 to 3.3 eV) is enhanced in Table 2. decreases in the energy gap refers to CdS nanofilm after doping with SnS and various thicknesses. This decrease in the energy gap could correspond to impurities that are not allowed from a result of production of secondary sites stages located in the energy gap that are near the conduction band. Thus, that may soak up and absorb photons of small energy. These results agreed with the same behavior in the literature [31].
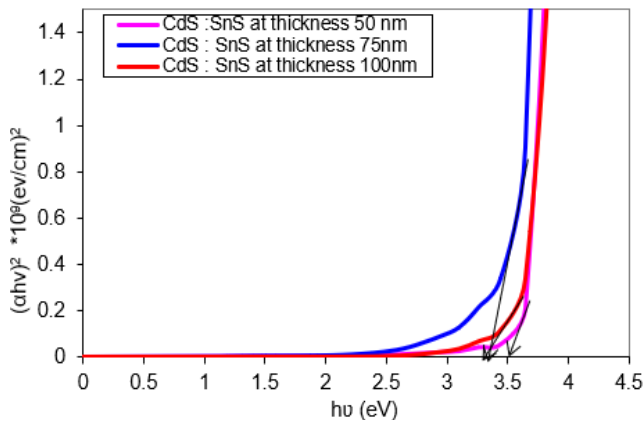

Figure 6. The scheme of $(\alpha h v)^2$ relative to Photon Energy (hv) for CdS:SnS with different Thicknesses

Table 2. CdS:SnS optical energy gap of nanofilms with different thicknesses

Films Type	Optical Energy Gap (eV)
CdS doping with SnS at a thickness of 50 nm	3.50
CdS doping with SnS at a thickness of 75 nm	3.35
CdS doping with SnS at a thickness of 100 nm	3.30

To get the linear absorption coefficient (α_o), the following formula was utilized:

$$\alpha_o = \frac{\ln\left(\frac{1}{T}\right)}{t} \qquad (3)$$

The transmittance represented as (T), and (t) is thickness while (n_o) refer to refractive index, which may be determined using the formula below from the film's transmittance spectrum [32]:

$$n_o = \frac{1}{T} + \left(\frac{1}{T^2} - 1\right)^{\frac{1}{2}} \qquad (4)$$

The proportion of light that travels through the solution is

known as transmittance. Therefore, the solution is considered to have 50% transmittance if half of the light is transferred [27].

$$T\% = \left(\frac{I}{I_o}\right) \times 100\% \qquad (5)$$

where, (I) intensity of light produced by the solvent and (I_o) intensity of the incoming beam of the light. The following formula represents the connection among transmittance (T) and absorbance (A) [33]:

$$A = \log 10\left(\frac{1}{T}\right) \qquad (6)$$

Utilize the following formula to get a refractive coefficient in nonlinear form by applies a normalized transmittance's peak-up to-dell variation [34]:

$$n_2 = \frac{\Delta\Phi_o}{I_o L_{eff} k} \qquad (7)$$

where, $k = 2\pi/\lambda$, (k) is wave number, (I_o) represents the intensity at the focal point and ($\Delta\Phi_o$) represented by shift the nonlinear phase.

To determine a nonlinear absorption coefficient (β) quickly, use the following Eq. (8) [35]:

$$\beta = \frac{2\sqrt{2}\, T(z)}{I_o L_{eff}} \qquad (8)$$

where, T(z): The focus point's minimum normalized transmittance value at (Z = 0).

4. Z-SCAN MEASUREMENTS

Z-Scan measurements were made in two parts: (open-closed) aperture. Every component was fabricated utilizing the constant wave (CW) pumped by diode solid state blue laser operative with wavelength (457) nm, the power (75) mW. For nonlinear refractive index was determined using a closed-aperture Z-Scan, whereas by using an open-aperture Z-Scan, for nonlinear absorption coefficient was determined. Using a convex lens, the beam was focused at (f =15) cm.

For focusing the beam of a leaser used convex lens applied to a sample and the beam waist was determined to be (0.025) cm at the focus, and the sample was transferring around the Z-axis. A sample transmittance used for function of sample location is measured. A technique shows symmetrized for fundamental and forward method for scan the refraction - absorption nonlinear. Appling single beam method is achieved by Gaussian beam that pass through the procedure of the sample motivated by the significant area. Via the Kerr scale the disturbance wavefront produce the self-focusing which lead to nonlinearity, the power passage a small crack.

For field far with differs which related to a sample location. Power production calculated according to the sample location, method deals with the (closed-open) cracks, as represented by Figure 7 [36].

4.1 Nonlinear refractive index of CdS

Figure 8(a) presents a Z-scan closed-aperture results in CdS

thin films with varying thicknesses (50, 75, and 100 nm). The nonlinear optical response is observed within the range of (–2 -+2) mm around the central point. The transmittance profile exhibits a characteristic peak-valley configuration, which showed the refractive index as a negative nonlinear ($n_2 < 0$), enhanced of self-defocusing behavior of examined films, which was summarized by Table 3. This nonlinear response contrasts with the linear regime, where the transmittance remains constant with sample displacement. However, under high-intensity illumination, the nonlinear refractive contribution becomes prominent, altering the beam propagation and confirming with third-order optical nonlinearity for CdS nanofilms, this agrees with the finding of researchers [37].
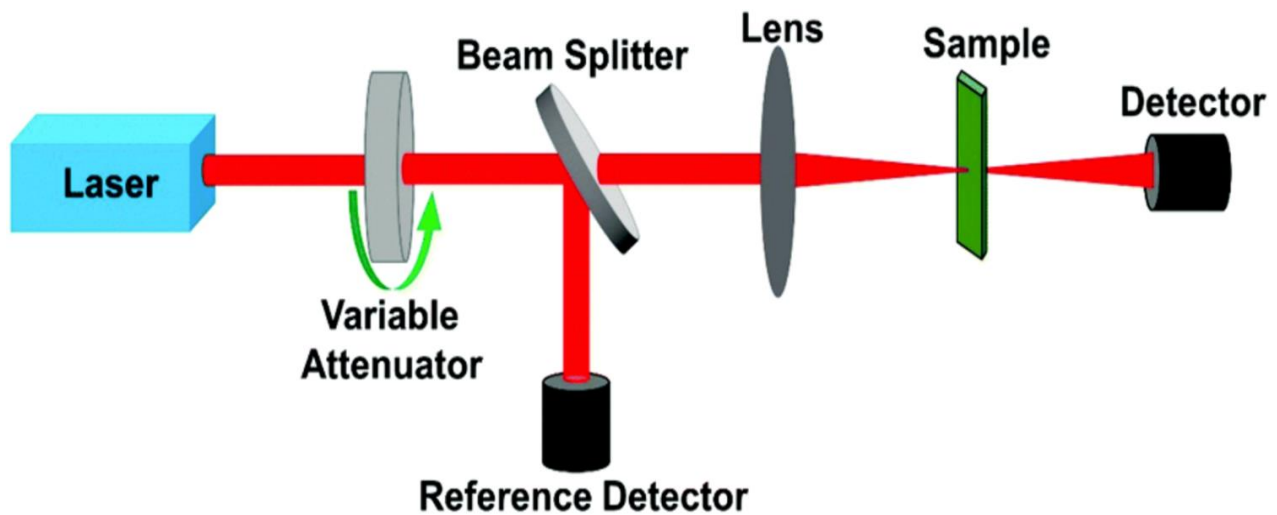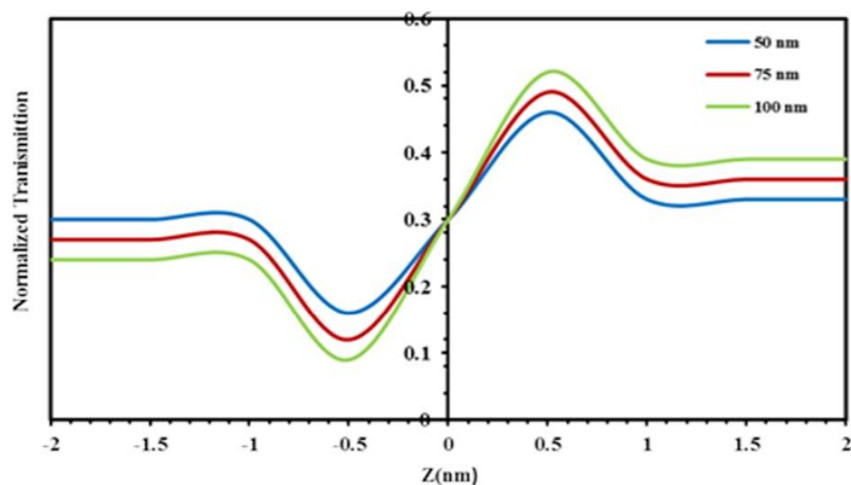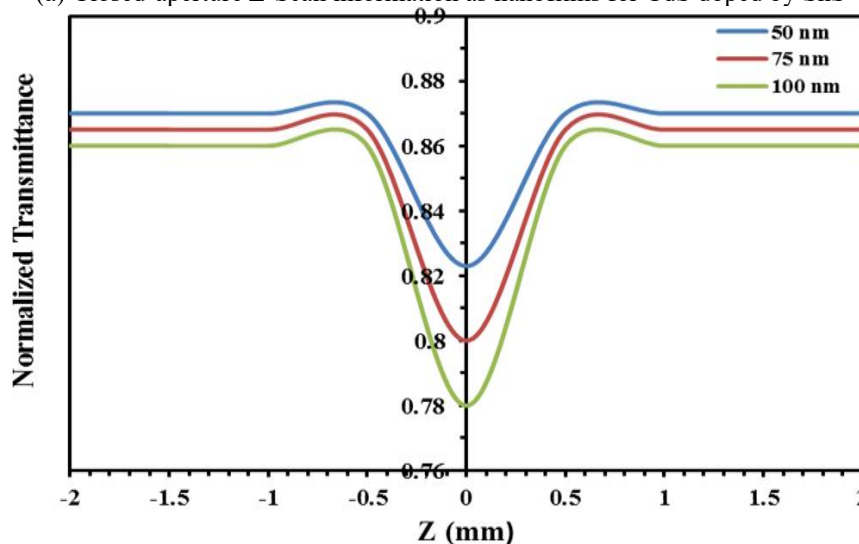

Figure 7. Closed and open-aperture (Z-Scan) [32]

(a) Closed-aperture Z-Scan information as nanofilms for CdS doped by SnS

(b) Open-aperture Z-Scan information as thin films of CdS doped with SnS

Figure 8. The information for Z-Scan (Closed-open) method due to nanofilms for CdS doped by SnS

4.2 Nonlinear absorption coefficient of CdS

Open-aperture Z-scan results stayed performed in the incident laser power of 70 mW for enhance a nonlinear optical characteristic of CdS nano films for various thicknesses (50, 75, and 100) nm were displayed in Figure 8. According to Figure 8(b), the transmittance curves exhibit a characteristic behavior associated with two-photon absorption (TPA). The transmittance increases gradually when the methods of sample with focal point (Z = 0 mm), then decreases to a minimum value (T_min), followed by a rise beyond the focal region. This trend clearly indicates the presence of nonlinear absorption near the beam waist. In regions far from the focal point (±Z), the transmittance remains essentially constant, reflecting linear optical behavior where the material response is independent of the light intensity. However, as the beam intensity increases near the focus, nonlinear effects become significant, leading to a measurable deviation from the linear regime, consistent with third-order nonlinearity in the CdS substrate. A nonlinear absorption coefficient (β) was computed by Eq. (6), and for nonlinear phase shift (φ) was derived from Eq. (5), as presented in Figure 8(b) and Table 3. The results reveal that increasing the film thickness enhances the nonlinear optical response, indicating a sturdy connection between the nanostructured films morphology and their light–matter interaction under high-intensity illumination this agree with references [37].

Table 3. The non-linear phase at Open-aperture Z-Scan information to nano films in CdS doped with SnS

Material	Thickness (nm)	ΔT_{P-v}	n_2 (cm²/mW)	T(z)	B (cm/mW)
	50	0.30	1.44×10^{-7}	0.82	2.68×10^{-3}
CdS:SnS	75	0.37	1.48×10^{-7}	0.80	2.34×10^{-3}
	100	0.43	1.70×10^{-7}	0.78	2.27×10^{-3}

Overall, these findings highlight the distinct contrast between the linear behavior of CdS films under low-intensity conditions and their pronounced nonlinear response near the focal point. This duality underscores the potential of CdS nanofilms to enhanced as nonlinear photonics with optical switching devices.

Z-scan behavior described as the figures, show beam strength of a transmittance changed and remained unceasing as the sample pass through from the focus. Rise in thickness becomes toward linear behavior for a sample position far field (+z). immediately, two-photon absorption seen when sample crossing the beam waist, will produce the intensity shifted. Which has agreement with findings of Jabbar et al. [12].

5. CONCLUSIONS

In CdS, different thicknesses of Nano films have been prepared. The goal of this work is based on a synthesis of CdS:SnS nanofilms, as shown by AFM data, which confirms that the surface smoothness was homogenous, whereas without affecting any cracks, it enhanced very essential for efficient charge transfer. Exposed, increasing the absorbance as the thickness of CdS increases. Makes the films more suitable for solar cell fabrication. The energy band gap (E_g) and all the coefficients have increased for the prepared films. For non-linear optical properties of CdS:SnS nanofilms, the findings show that the absorbance rose for the same wavelength as the thicknesses increased. The absorption non-linear factor and the refraction non-linear index for CdS:SnS nanofilms, it measured by the Z-Scan method, has widely sensitive technique, showed that the nonlinear refractive index rose as powers increased for all generated samples, whereas the nonlinear absorption coefficient declined. Compared to pure CdS, CdS:SnS nanofilms have shown better optical limiting and nonlinear properties. Two assumptions are exposed: one assumes refers to the unique characterization of a Nano film, where it is revealed according to their thickness, whereas the second shows that by applying the method of thermal evaporation exhibit strong interfacial properties to produce the CdS Nano films. The findings suggest that CdS:SnS nanofilms are very proper to producing of photovoltaic cells like a solar concentrator for enhancing it performance via promoting widely space for solar spectrum to cell to produce electricity. Reviewing the nonlinear optical characterization for these materials by applying a different wavelengths laser.

AUTHORS' CONTRIBUTIONS

REFERENCES

[1] Saravanan, A., Kumar, P.S., Karishma, S., Vo, D.V.N., Jeevanantham, S., Yaashikaa, P.R., George, C.S. (2021). A review on biosynthesis of metal nanoparticles and its environmental applications. Chemosphere, 264: 128580. https://doi.org/10.1016/j.chemosphere.2020.128580

[2] Shkir, M., Ashraf, I.M., Khan, A., Khan, M.T., El-Toni, A.M., AlFaify, S. (2020). A facile spray pyrolysis fabrication of Sm: CdS thin films for high-performance photodetector applications. Sensors and Actuators A: Physical, 306: 111952. https://doi.org/10.1016/j.sna.2020.111952

[3] Abass, K.H., Adil, A., Alrubaie, A.J., Rabee, B.H., Kadim, A.M., Talib, S.H., Mohammed, K.A., Jassim, A.S. (2023). Fabrication and characterization of p-SnS/n-Si solar cell by thermal evaporation technique and the effect of ag-doped on its efficiency. International Journal of Nanoscience, 22(01): 2350003. https://doi.org/10.1142/S0219581X23500035

[4] Abass, K.H., Adil, A., Mohammed, M.K. (2018). Fabrication and enhancement of SnS: Ag/Si solar cell via thermal evaporation technique. Journal of Engineering and Applied Sciences, 13(4): 919-925. https://ijisae.org/index.php/IJISAE/article/view/3662.

[5] Yılmaz, S., Töreli, S.B., Polat, İ., Olgar, M.A., Tomakin, M., Bacaksız, E. (2017). Enhancement in the optical and electrical properties of CdS thin films through Ga and K co-doping. Materials Science in Semiconductor Processing, 60: 45-52. https://doi.org/10.1016/j.mssp.2016.12.016

[6] Attia, A.A., Hashim, F.S., Abass, K.H. (2023). Solar cell of Sb2O3: CuO/Si prepared via thermal evaporation technique: Structural, morphological properties and efficiency. Canadian Journal of Chemistry, 101(10): 813-820. https://doi.org/10.1139/cjc-2023-0001

[7] Attia, A.A., Hashim, F.S., Abass, K.H. (2023). Fabrication and characterization of p-Sb2O3: CuO/n-Si solar cell via thermal evaporation technique. International Journal of Nanoscience, 22(3): 2350023. https://doi.org/10.1142/S0219581X23500230

[8] Akter, M., Khan, M.N.I., Mamur, H., Bhuiyan, M.R.A. (2020). Synthesis and characterisation of CdSe QDs by using a chemical solution route. Micro & Nano Letters, 15(5): 287-290. https://doi.org/10.1049/mnl.2019.0200

[9] Abass, K.H., Latif, D.M. (2016). The urbach energy and dispersion parameters dependence of substrate temperature of CdO thin films prepared by chemical spray pyrolysis. International Journal of ChemTech Research, 9(9): 332-338. https://doi.org/10.1063/5.0095169

[10] Handique, K.C., Kalita, P.K., Barman, B., Das, H. (2024). Photo-induced single-electron tunnelling based Coulomb staircase effect observed at high applied bias in ZnSe/CdSe core-shell quantum dots. Optical and Quantum Electronics, 56(3): 357. https://doi.org/10.1007/s11082-023-05920-4

[11] Talapin, D.V., Shevchenko, E.V., Kornowski, A., Gaponik, N., Haase, M., Rogach, A.L., Weller, H. (2001). A new approach to crystallization of CdSe nanoparticles into ordered three-dimensional superlattices. Advanced Materials, 13(24): 1868-1871. https://doi.org/10.1002/1521-4095(200112)13:24%3C1868::AID-ADMA1868%3E3.0.CO;2-0

[12] Jabbar, S.A., Naser, B.A., Mahdi, S.A. (2024). Non-linear and linear optical properties of an organic laser dye mixture. Revue des Composites et des Matériaux Avancés-Journal of Composite and Advanced Materials, 34(4): 401-407. https://doi.org/10.18280/rcma.340401

[13] Tang, Z., Zhang, Z., Wang, Y., Glotzer, S.C., Kotov, N.A. (2006). Self-assembly of CdTe nanocrystals into free-floating sheets. Science, 314(5797): 274-278. https://doi.org/10.1126/science.1128045

[14] Handique, K.C., Kalita, P.K. (2020). Effects of cadmium ion concentration on the optical and photo-response properties of CdSe/PVP nanocomposites for white light sensing application. Applied Physics A, 126(9): 755. https://doi.org/10.1007/s00339-020-03934-3

[15] Srivastava, S., Santos, A., Critchley, K., Kim, K.S., et al. (2010). Light-controlled self-assembly of semiconductor nanoparticles into twisted ribbons. Science, 327(5971): 1355-1359. https://doi.org/10.1126/science.1177218

[16] Chen, Y.Y., Chen, D.D., Li, Z., Peng, X.G. (2017). Symmetry-breaking for formation of rectangular CdSe two-dimensional nanocrystals in zinc-blende structure. Journal of the American Chemical Society, 139(29): 10009-10019. https://doi.org/10.1021/jacs.7b04855

[17] Sabah, A., Shafaqat, I., Naifar, A., Albalawi, H., Alqahtani, M.S., Ashiq, M.G.B., Shabbir, S.A. (2023). Investigation of band parameters and electrochemical analysis of multi core-shell CdSe/CdS/ZnS quantum dots. Optical Materials, 142: 114065. https://doi.org/10.1016/j.optmat.2023.114065

[18] Yılmaz, S. (2015). The investigation of spray pyrolysis grown CdS thin films doped with flourine atoms. Applied Surface Science, 357: 873-879. https://doi.org/10.1016/j.apsusc.2015.09.098

[19] Punitha, K., Sivakumar, R., Sanjeeviraja, C., Ganesan, V. (2015). Influence of post-deposition heat treatment on optical properties derived from UV－vis of cadmium telluride (CdTe) thin films deposited on amorphous substrate. Applied Surface Science, 344: 89-100. https://doi.org/10.1016/j.apsusc.2015.03.095

[20] Liu, B., Luo, R., Li, B., Zhang, J.Q., Li, W., Wu, L.L., Feng, L.H., Wu, J. (2016). Effects of deposition temperature and CdCl2 annealing on the CdS thin films prepared by pulsed laser deposition. Journal of Alloys and Compounds, 654: 333-339. https://doi.org/10.1016/j.jallcom.2015.08.247

[21] Yücel, E., Yücel, Y., Durak, M. (2017). Optimization of growth parameters for absorber material SnS thin films grown by SILAR method using response surface methodology. Journal of Materials Science: Materials in Electronics, 28: 2206-2214. https://doi.org/10.1007/s10854-016-5788-3

[22] Hennayaka, H.M.M.N., Lee, H.S. (2014). Effect of rapid thermal annealing on the microstructural and optical properties of electrodeposited SnS thin films. Electronic Materials Letters, 10: 217-221. https://doi.org/10.1007/s13391-013-3040-3

[23] Liu, D., Feng, J., Tian, M., Li, Q., Sa, R. (2021). First-principles study of the stability, electronic and optical properties of CdTe under hydrostatic pressure. Chemical Physics Letters, 764: 138272. https://doi.org/10.1016/j.cplett.2020.138272

[24] Fathy, M., Elyamny, S., Mahmoud, S., Kashyout, A E.H.B. (2015). Effect of thermal and chemical treatment on electrodeposited CdTe thin films for solar cell applications. International Journal of Electrochemical Science, 10(8): 6030-6043. https://doi.org/10.1016/S1452-3981(23)06700-7

[25] Nieto-Zepeda, K.E., Guillén-Cervantes, A., Rodríguez-Rosales, K., Santos-Cruz, J., et al. (2017). Effect of the sulfur and fluorine concentration on physical properties of CdS films grown by chemical bath deposition. Results in Physics, 7: 1971-1975. https://doi.org/10.1016/j.rinp.2017.06.008

[26] Kazem, G.A., Saeed, M.H. (2012). Influence of substrate temperature on optical properties of cdo thin films. Journal of the College of Basic Education, 18(73): 135-146. https://doi.org/10.35950/cbej.v18i73.9199

[27] Naser, B.A., Abd Ulkadhem, N.J., Mousa, A.O. (2020). Effect of solvents on linear optical properties for nematic liquid crystals. In IOP Conference Series: Materials Science and Engineering, Thi-Qar, Iraq, 928(7): 072055. https://doi.org/0.1088/1757-899X/928/7/072055

[28] Subramanian, B., Sanjeeviraja, C., Jayachandran, M. (2001). Cathodic electrodeposition and analysis of SnS films for photoelectrochemical cells. Materials Chemistry and Physics, 71(1): 40-46. https://doi.org/10.1016/S0254-0584(00)00526-5

[29] Jabbar, S.A., Mahdi, S.A., Naser, B.A. (2025). Nonlinear optical characteristics of thin films made from mixed organic laser dyes doped with metal nanoparticles and PMMA polymer. Iraqi Journal of Applied Physics, 21(1): 121-126.

[30] Tauc, J., Menth, A., Wood, D.L. (1970). Optical and magnetic investigations of the localized states in semiconducting glasses. Physical Review Letters, 25(11): 749. https://doi.org/10.1103/PhysRevLett.25.749

[31] Jabbar, S.A., Naser, B.A., Mahdi, S.A. (2024). Spectral and linear optical properties for new mixture of Nile Blue and Malachite Green organic laser dyes. Instrumentation Mesure Métrologie, 23(5): 383-389. https://doi.org/10.18280/i2m.230506

[32] Chen, J.S., Zhang, W., Pullerits, T. (2022). Two-photon absorption in halide perovskites and their applications. Materials Horizons, 9(9): 2255-2287. https://doi.org/10.1039/D1MH02074A

[33] Patil, P.S., Maidur, S.R., Rao, S.V., Dharmaprakash, S.M. (2016). Crystalline perfection, third-order nonlinear optical properties and optical limiting studies of 3, 4-Dimethoxy-4'─methoxychalcone single crystal. Optics & Laser Technology, 81: 70-76. https://doi.org/10.1016/j.optlastec.2016.01.033

[34] Altaify, D.O., Mahdi, Z.F. (2007). Nonlinear optical properties of CdS thin film nanoparticles using z-Scan technique. Iraqi Journal of Laser, Part A(6): 9-14. https://doi.org/10.31900/ijl.v6iA.133

[35] Mohamed, Z.Q., Al-Ogaili, A.O.M., Abass, K.H. (2023). Morphology and optical properties of Cu2O-Doped CuO nano films prepared via thermal evaporation technique. In AIP Conference Proceedings, Diyala, Iraq, 2475: 090037. https://doi.org/10.1063/5.0102570

[36] Qassim, Z., Mousa Al-Ogaili, A.O., Haneen Abass, K. (2024). Enhancement of CuO/Si Solar cell efficiency by Cu2O doping prepared via thermal evaporation technique. Nano, 19(14): 2450085. https://doi.org/10.1142/S1793292024500851

[37] Qassim, Z., Al-Ogaili, A.O.M., Abass, K.H. (2022). Morphology of copper oxide nano-layer prepared via thermal evaporation technique. NeuroQuantology, 20(3): 87-94. https://doi.org/10.14704/nq.2022.20.3.NQ22046